JGR Oceans

RESEARCH ARTICLE
10.1029/2020JC016507

A Survival Analysis of the Gulf Stream Warm Core Rings

E. Nishchitha S. Silva[1,2], Avijit Gangopadhyay[1], Gavin Fay[1], Manushi K. V. Welandawe[3,4], Glen Gawarkiewicz[5], Adrienne M. Silver[1], Mahmud Monim[6], and Jenifer Clark[7]

[1]School for Marine Science and Technology, University of Massachusetts Dartmouth, Dartmouth, MA, USA, [2]Department of Earth and Environment, Boston University, Boston, MA, USA, [3]Department of Computer Science and Statistics, University of Rhode Island, South Kingstown, RI, USA, [4]Department of Mathematics and Statistics, Boston University, Boston, MA, USA, [5]Woods Hole Oceanographic Institution, Woods Hole, MA, USA, [6]RPS Group, South Kingstown, RI, USA, [7]Jenifer Clark's Gulfstream, Dunkirk, MD, USA

Abstract Survival of Gulf Stream (GS) warm core rings (WCRs) was investigated using a census consisting of a total of 961 rings formed during the period 1980–2017. Kaplan-Meier survival probability and Cox hazard proportional models were used for the analysis. The survival analysis was performed for rings formed in four 5° zones between 75° W and 55° W. The radius, latitude, and distance from the shelf-break of a WCR at formation all had a significant effect on the survival of WCRs. A pattern of higher survival was observed in WCRs formed in Zone 2 (70°–65° W) or Zone 3 (65°–60° W) and then demised in Zone 1 (75°–70° W). Survival probability of the WCRs increased to more than 70% for those formed within a latitude band from 39.5° to 41.5° N. Survival probability is reduced when the WCRs are formed near the New England Seamounts.

Plain Language Summary The Gulf Stream produces warm core rings in the Western Atlantic Ocean due to its meandering nature. These warm core rings have physical, chemical, and biological impacts on shelf and slope sea regions of the Western North Atlantic. This region is one of the most highly productive fishing areas in the world, and there is a need to understand the Warm Core Ring influence on different food web systems. We use data from a 38-yearlong (1980–2017) warm core ring census to investigate the survival probability of these warm core rings. After using multiple survival analysis techniques (a popular analysis technique in the medical and health sciences), we observed a high survival probability in WCRs formed within the 7°–65° W longitudinal band. Also, the warm core rings which demised within the 75°–70° W longitudinal band exhibited higher survival. The effect of the New England Seamount Chain (NESC) on WCR survival probabilities was revealed through a Cox proportional hazard model which showed that the further east a ring was formed from the NESC, the higher the survival probability. These findings are very important as precursors to understand the effect of WCRs on shelf-slope processes in the Western North Atlantic.

Key Points:
- Survival of Gulf Stream warm core rings was analyzed using Kaplan-Meier and Cox Hazard proportional models
- Ring survival depends on the zone, season, latitude, and proximity to New England Seamount at formation
- A pattern of higher survival was observed for rings formed within 70°–65° W and then demised within 75°–70° W

Correspondence to:
E. N. S. Silva,
netige@bu.edu

Citation:
Silva, E. N. S., Gangopadhyay, A., Fay, G., Welandawe, M. K. V., Gawarkiewicz, G., Silver, A. M., et al. (2020). A survival analysis of the Gulf Stream warm core rings. *Journal of Geophysical Research: Oceans*, *125*, e2020JC016507. https://doi.org/10.1029/2020JC016507

Received 15 JUN 2020
Accepted 6 OCT 2020
Accepted article online 14 OCT 2020

1. Introduction

As the western boundary current of the subtropical North Atlantic Gyre, the Gulf Stream (GS) plays a major role in transporting heat and salt toward North Atlantic polar regions. Warm core rings (WCRs) are anti-cyclonic mesoscale eddies that pinch off from the stream as a result of high-amplitude meandering. Such high-amplitude meandering occurs once the GS detaches from the coast at Cape Hatteras to the deeper ocean from its shore parallel pathway along the eastern continental shelf margin of the United States. WCRs are a major driver of changes in the shelf and slope waters of the U.S. northeast, as they provide the latitudinal excursion of warmer waters (Bisagni, 1983; Gawarkiewicz et al., 2001; Joyce & McDougall, 1992; Ramp et al., 1983). The frequent occurrence of WCRs and their impact on the physical, chemical, and biological oceanography of the Slope Sea region have been documented through field observations (Joyce, 1985; Lai & Richardson, 1977; Saunders, 1971), satellite imagery (Auer, 1987; Bisagni, 1976; Brown et al., 1986; Halliwell & Mooers, 1979) and analyzed using theoretical and diagnostic models (Csanady, 1979; Flierl, 1977).

WCRs are unique ecotones that are composed of water masses from the Sargasso Sea and the GS. They create distinctive biological regions in the slope water due to the locomotion of Sargasso water to the slope sea. Information on biological communities in ocean eddies was reviewed in Olson (1991). The biological

composition of rings is decided by the parent water mass in the core of the ring, season of formation that is related to the annual cycle of the parent waters, and ring dynamics and intrusion of communities through time. Joyce and Wiebe (1983) reported an observed WCR having deep mixed Sargasso water in the core. This nutrient-poor core water later developed a thermal stratification leading to a spring bloom. Zooplankton communities in a core of a WCR vary with the seasonality and ability of zooplankton to survive as seed populations during the evolution of a ring (Davis & Wiebe, 1985; Wiebe et al., 1985). WCRs have also been hypothesized to be a mode of northward larval transport (Cowen et al., 1993; Hare et al., 2002). The survival of larvae and type of larvae that are transported depend on both ring age and formation location.

The present study was carried out following the development of a 38-yearlong census of the WCRs (Gangopadhyay & Gawarkiewicz 2020) and the results of a number of related recent studies (Gangopadhyay et al., 2019; Gangopadhyay, Gawarkiewicz, Silva, et al., 2020; Monim, 2017; Silva, 2019) using the census data. These systematic studies on the GS WCR formation and distribution characteristics highlighted the critical need of investigating the dependence of the longevity of WCRs on various factors including their locations of formation and demise, and the seasons and size at formation.

A clear regime shift in WCR formation was observed around the year 2000 and was reported by Gangopadhyay et al. (2019). The WCR formation over the whole region (75°–55° W) increased from an average of 18 per year during Regime 1 (1980–1999) to 33 per year during Regime 2 (2000–2017). For geographic analysis, formation locations were grouped in four 5° zones between 75 and 55° W: Zone 1 (75°–70° W), Zone 2 (70°–65° W), Zone 3 (65°–60° W), and Zone 4 (60°–55° W). See Figure 1 (upper panel). This zoning stems from two factors. First, the GS is shown to be responding with different temporal variability (on both interannual and secular time scales) to the east and west of 65–60° W (Zone 3) (Gangopadhyay et al., 2016; Bisagni et al., 2017). Second, further geographic perspective provides more information on ring formation dynamics for two reasons: (i) Zone 1 (75°–70° W) is generally a standing meander pattern for the GS with less ring activity; (ii) the New England Seamount Chain (NESC) underlies the GS between 65° and 60° W (Zone 3), thus creating large-amplitude meanders after 60° W with frequent WCR formation to the east. Seasonally, WCR formations show significant summer maxima and winter minima, a pattern that is consistent through all zones and both temporal regimes.

An extended statistical analysis of the WCR census focused on the variability of formation, lifespan, and size of the rings (Gangopadhyay, Gawarkiewicz, Silva, et al., 2020). Major relevant results include the following: (i) The lifespan and size distribution show progressively more rings with higher longevity and greater size when formed to the east of 70° W, and (ii) the average lifespan of the WCRs in all four zones decreased by 20–40% depending on zones and/or seasons from Regimes 1 to 2. Figure 1 (middle and bottom panels) presents a summary of results from the 961 WCRs analyzed on the zonal distribution of formation and demise.

Understanding the physical survival of WCRs is critical for predicting ecosystem responses at multiple trophic levels along the coasts of the United States and Canada. Early work by McCarthy and Nevins (1986) and references therein and more recent work by Gaube and McGillicuddy (2017) highlight not only the important influence WCRs can have on nutrient levels and primary productivity but also how these relationships change with ring age. Generally, newly formed WCRs have lower nutrients and primary productivity than the older WCRs. Thus, the survival of a ring could be directly linked to the nutrient availability and primary productivity and affect the food supply chain of the ecosystem for multiple species.

When WCRs hit the shelf, they can trigger a subsurface exchange of shelf and slope water with near-surface slope water moving onshore and near bottom shelf water being drawn around the ring. This exchange is significant in affecting the salt balance of Middle Atlantic Bight Shelf Water (Churchill et al., 1986). Along with its effect on salinity, this exchange process can affect the larval abundance of shelf species by shelf water entrainment into the ring, transporting the larva to unfavorable conditions in the slope waters (Flierl & Wroblewski, 1984; Myers & Drinkwater, 1986; Smith et al., 1979).

The 38-year long unique census of the WCRs (Gangopadhyay & Gawarkiewicz, 2020) allowed us to investigate the persistence of these rings using the survival analysis methods. Survival analysis, a popular data analysis method in the field of medical statistics, involves investigating the survival probabilities of certain populations based on time to an event (Kleinbaum & Klein, 2012). WCRs have a similar population characteristic in that from the time of formation they have a lifetime until they demise.

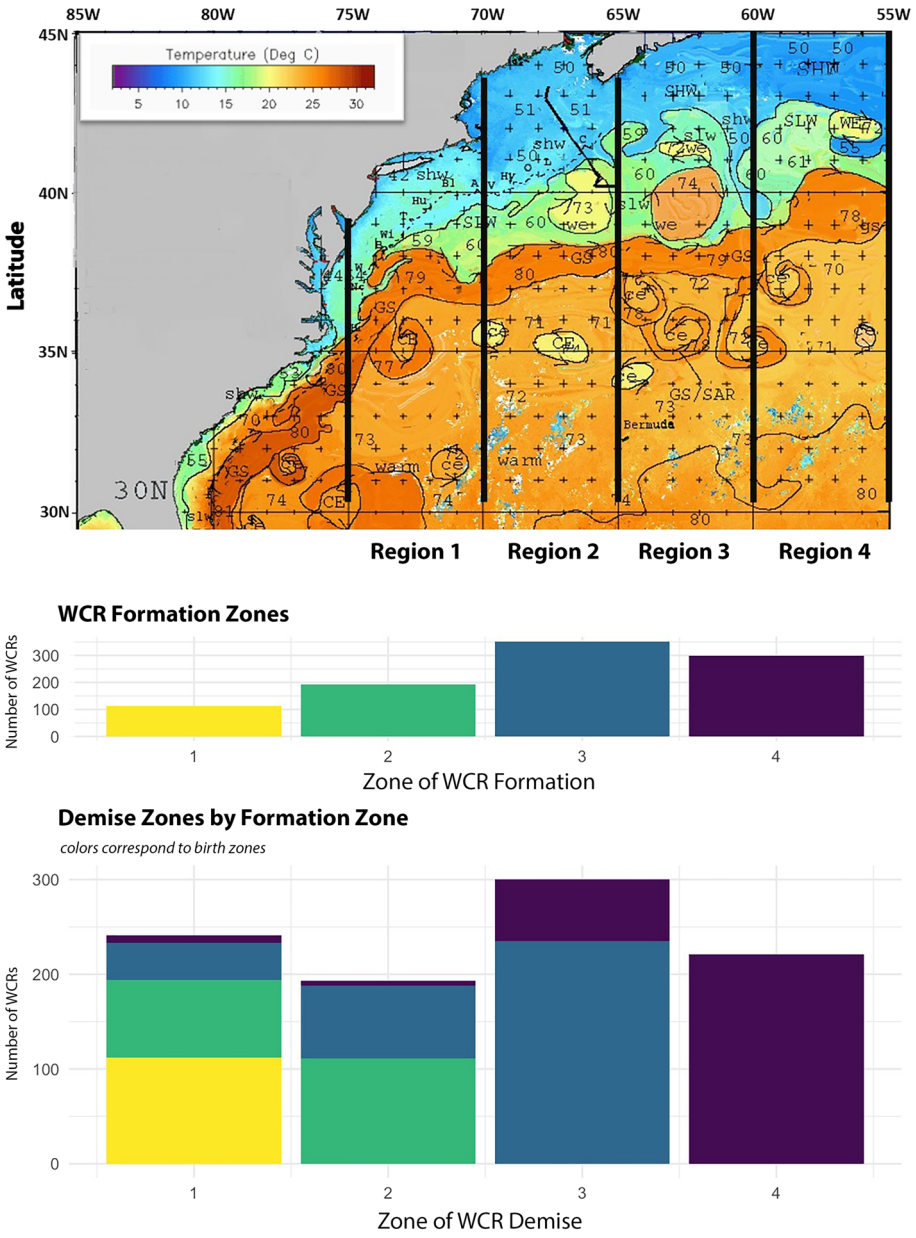

Figure 1. Upper panel: domain of study showing four different zones. Demarcating lines represent different features in the domain, colors refer to temperature in degrees Celsius, and numbers on the map are temperature in degrees Fahrenheit. Middle and bottom panels: formation and demise of WCRs formed in different zones.

The basic goals of survival analysis are (i) to estimate and interpret survivor and or hazard function from the survival data, (ii) to compare survival and/or hazard functions, and (iii) to assess the relationship of explanatory variables to survival time (Kleinbaum & Klein, 2012). There are three major components of survival analysis—time, event, and censoring. The time component maybe seconds, days, or years based on the nature of a study and its subjects. It is the time until the event occurs and is the outcome variable. The event may be a death, or a disease incident, or any designated experience of interest that may happen to an individual. Censoring is included in the analysis when no survival information of an individual in the study is available. For WCRs, the event is the demise of a WCR, and time is the lifespan of a WCR from its formation to demise. Censoring was not necessary due to the complete nature of WCR survival data. The overall goal of this study is to explore the survival probability of GS WCRs by considering the lifespan of WCRs as the response variable. This was achieved by applying important WCR characteristics to multiple survival models while analyzing them individually as well as collectively.

The outline of the paper is as follows. Section 2 briefly describes the WCR data and the survival analysis methodology. Section 3 documents the survival functions for the different groups of WCRs based on their geographic and temporal categories. Section 4 presents the results from the Cox model showing the impact of different hazards on the risk of failure of the WCRs. Section 5 discusses the results followed by a conclusion in section 6.

2. Data and Methods

2.1. Data

The primary data set of this study was the census (1980–2017) created from a set of GS analysis charts prepared by coauthor Jenifer Clark (Gangopadhyay & Gawarkiewicz, 2020; Monim, 2017; Silva, 2019). These GS charts are a synoptic chart series extending from 1980 to present. The basis data source for the Jenifer Clark (JC) charts was individual infrared temperature images from the NOAA polar orbiting satellites (NOAA-5 in the early 1980s to NOAA-18 recently) at 6- to 12-hr intervals. These images were captured by the Advanced Very High Resolution Radiometer (AVHRR) and AVHRR2 instruments, which had a resolution of 1.1 km. Each image has a different lookup table (or colormap) for temperature that resolves 256 distinct sets of intensity, hue, and saturation of color within the available and retrievable IR signal range. This allows for accurate identification of the small-scale features in each image. Please see Gangopadhyay et al. (2019) for a detailed description of GS charts generation. These charts dynamically document the GS signature and its rings two to three times each week. Charts have been produced and used by National Oceanic and Atmospheric Administration (NOAA) during 1980–1994 for the purpose of operational applications by the U.S. Navy, fishermen, sailboats, oceanographic modelers, oil/gas exploration industries, and weather forecasters.

These JC charts were georeferenced and added to a Geographical Information System (GIS) data frame (Decker, 1986; QGIS Development Team, 2016). Within the GIS data frame, an analyst examined each chart following the WCR formation, continuity, and dissipation rules. A new ring formation is documented in three situations: (i) a typical GS crest forming a closed anticyclonic vortex and detaches from the stream in the slope water; (ii) an anticyclonic eddy forms off of another large anticyclonic eddy in the slope water; and (iii) an anticyclonic eddy further away from the stream coming into the domain through Zone 4 (Gangopadhyay, Gawarkiewicz, Silva, et al., 2020). The demise of a ring is decided when a ring was last documented (or seen) in the JC charts. If any new ring formed and persisted for at least 7 days, the ring was documented by digitizing the shape to obtain the centroid along with the formation coordinates. Subsequently, the last documented location and date for each WCR were recorded in the census. To avoid capturing the smaller isolated rings which may appear and disappear during interactions with the GS or the shelf break, the census analyst revisits the census data against the observed JC charts sequentially and repetitively during the process of finalizing an annual census. For example, while checking the newly created annual census, the analyst checks for sudden appearances of new WCRs that appeared without any prior evolution of GS meandering or appearance of other ring formation processes. These WCRs are then identified as previously disappeared and reappeared WCRs and reinserted in the charts within the disappearing window.

For each newly formed WCR, the outline of the WCR was digitized, and the area was calculated using GIS (QGIS Development Team, 2016). Based on the WCR area, an equivalent radius (R) was calculated, where $R = \sqrt{WCRArea/\pi}$. This method is similar to the one used by Brown et al. (1983) except that we used the GIS-derived area of the WCR instead of the ellipse fit method used by them. For further details on size calculation, please see Gangopadhyay et al. (2019), Monim (2017), and Silva (2019). The area information of all 961 rings are provided with the census data (Gangopadhyay & Gawarkiewicz, 2020). The time duration between a WCR formation and its demise is the lifespan or the total survival time of a WCR. It is the difference between the date of absorption (DOA) and the date of birth (DOB) of a WCR (refer to Table 1 of Gangopadhyay, Gawarkiewicz, Silva, et al., 2020). The master data set of these aforementioned annual WCR censuses, which consisted of 961 GS WCRs for the period 1980 to 2017 (Gangopadhyay & Gawarkiewicz, 2020), was used for the survival analysis. A detailed description of the WCR census development is presented in Gangopadhyay, Gawarkiewicz, Silva, et al. (2020).

2.2. Survival Analysis Methodology

The survival analysis methods we applied can be described as a two-step process. In the first step, the available data were processed to derive the survival curve or the survival function. In our case, this was done by

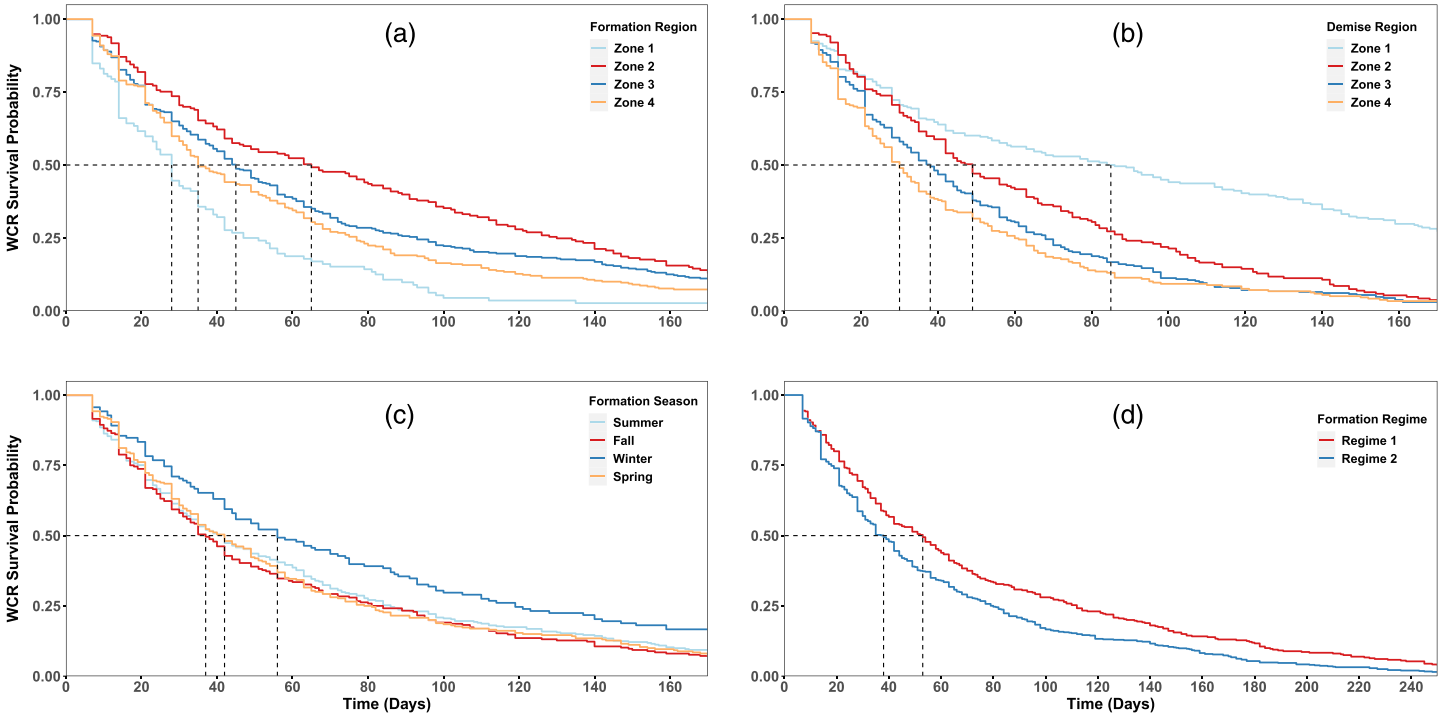

Figure 2. Survival probability of warm core rings over time for different geographic and temporal cohorts. Survival curves for WCRs grouped by (a) their zone of formation (top left); (b) their zone of demise (top right); (c) their season of formation (bottom left); and (d) regimes for the whole region where Regime 1 is (1980–1999) and Regime 2 is (2000–2017) (bottom right). The dashed horizontal line in each panel is the baseline indicator for the probability of 0.5. The dashed vertical line for each survival curve then indicates the lifespan when the survival probability is 50%.

analyzing the 961 WCRs and their lifespan, grouped into selected geographic and temporal bins. In the second step, a set of Cox models were fit to the data in these same groupings, to estimate the magnitude of the effects of conceived hazards for the risk of failure of the group of WCRs.

The probability function which describes the survival of a population is called the survivor/survival function $S(t)$. The survival function is given by

$$S(t) = P(T \geq t) = \int_t^{\infty} f(x)dx, \tag{1}$$

where probability (P) of an event occurring after a time point (t). T is the failure time, and $f(x)$ is the probability density function of T. In the context of WCRs, it is the probability of WCRs surviving after time t. In theory, the survivor function is a smooth curve starting from a probability of 1 and then decreasing toward zero with time. In practice, the survival function is often a step function since the time variable is discrete in practical studies (Kleinbaum & Klein, 2012). The survival function is fundamental to a survival analysis since obtaining survival probabilities for different values of t provides crucial summary information from survival data (Clark et al., 2003).

The discrete Kaplan-Meier (KM) estimator (Kaplan & Meier, 1958) was used to estimate the survival function of GS WCRs. The mathematical formulation of the KM estimator is

$$S(t_i) = \prod_{i:t_i \leq t} (1 - \frac{d_i}{n_i}), \tag{2}$$

where t_i is time at least one event happens, d_i is the number of events that happened at time t_i, and n_i is surviving individuals at t_i.

Log-rank tests were used to compare survival curves (Figure 2) generated by subsetting GS WCRs into multiple groups based on their zones of formation and demise, seasons of formation and demise, and the regime of formation (before or after the year 2000). A log-rank test determines the statistical equivalency of KM

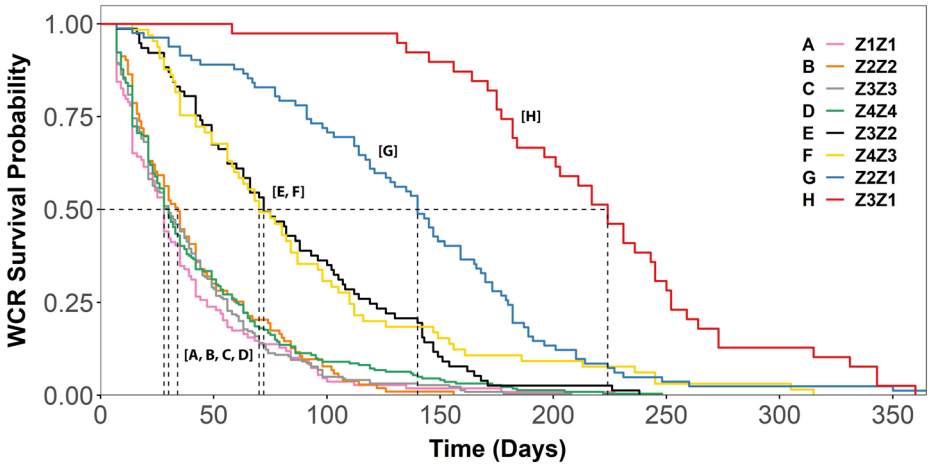

Figure 3. Survival function of GS WCRs for different formation and demise zone combination (*ZxZy*: x = formation zone, and y = demise zone). Survival curves are binned into three categories; WCRs formed in and demised in the same zone (A–D), WCRs with Z3Z2 and Z4Z3 combinations (E and F), and WCRs with Z3Z1 and Z2Z1 combination (G and H).

curves (Kleinbaum & Klein, 2012). It is a large sample chi-square test where the null hypothesis (H_0) states that all survival curves are the same. The equation for the log-rank test is

$$\chi^2 = \sum_{i}^{\#\text{ of groups}} \frac{(O_i - E_i)^2}{E_i}, \tag{3}$$

where O_i is the observed and E_i is the expected number of events in each group. The analysis was conducted using the R software's (R Core Team, 2018) survival package (Therneau, 2015). Together with Figure 2 and Equations 1 to 3, this completes the first step of the two-step methodology. The results from Step 1 analysis is presented in Figure 3 and discussed later in section 3.

For the second step, the hazard function $h(t)$ is the instantaneous potential per unit time for an event to occur given that the individual has survived up to time t. For an example, if a WCR persisted until time t, the rate of instantaneous hazard/risk of failing/demising of the WCR is given by $h(t)$. Note that while they are conceptually and mathematically related, $S(t)$ is always focused on survival while $h(t)$ focuses on the potential of failing. Also, $h(t)$ is a rate where the scale ranges from 0 to infinity while $S(t)$ is a probability ranges from 1 to 0. The mathematical formulation of $h(t)$ is

$$h(t) = \lim_{\Delta t \to 0} \frac{P(t \le T < t + \Delta t | T \ge t)}{\Delta t}, \tag{4}$$

where Δt is a small interval of time considered. The importance of $h(t)$ is that it can be used to identify specific model forms (e.g., exponential, Weibull, and log normal) that are best fit for the data. It can also be used for mathematical modeling of survival data (Kleinbaum & Klein, 2012). Therefore, survival models are often written in terms of $h(t)$.

We evaluated the risk of WCR failure for a number of hazard factors by constructing a number of Cox proportional hazard (PH) models (Cox & Oakes, 1984). The reasoning for choosing the Cox model is that we did not have to assume any particular distribution model for the WCR lifespan distribution a priori. Cox model is a semiparametric model since its baseline hazard is an unspecified function (i.e., we do not assume a distribution for the baseline hazard). Even though the Cox model is a semiparametric model, it has the ability to provide good estimates of regression coefficients and hazard ratios of interest for a wide variety of data situations.

The general formulation of a Cox model is shown in Equations 4 and 5, where $h_i(t|\mathbf{x}_i)$ denotes the hazard function given the covariates $\mathbf{x}_i = (x_{i1}, \ldots, x_{ip})^T$ of the ith observation, $h_0(t)$ is the baseline hazard, and $\boldsymbol{\beta} = (\beta_0, \ldots, \beta_p)$ denotes the vector of the regression coefficients.

$$h_i(t|\mathbf{x}_i) = h_0(t)e^{(\boldsymbol{\beta}\mathbf{x}_i)}, \tag{5}$$

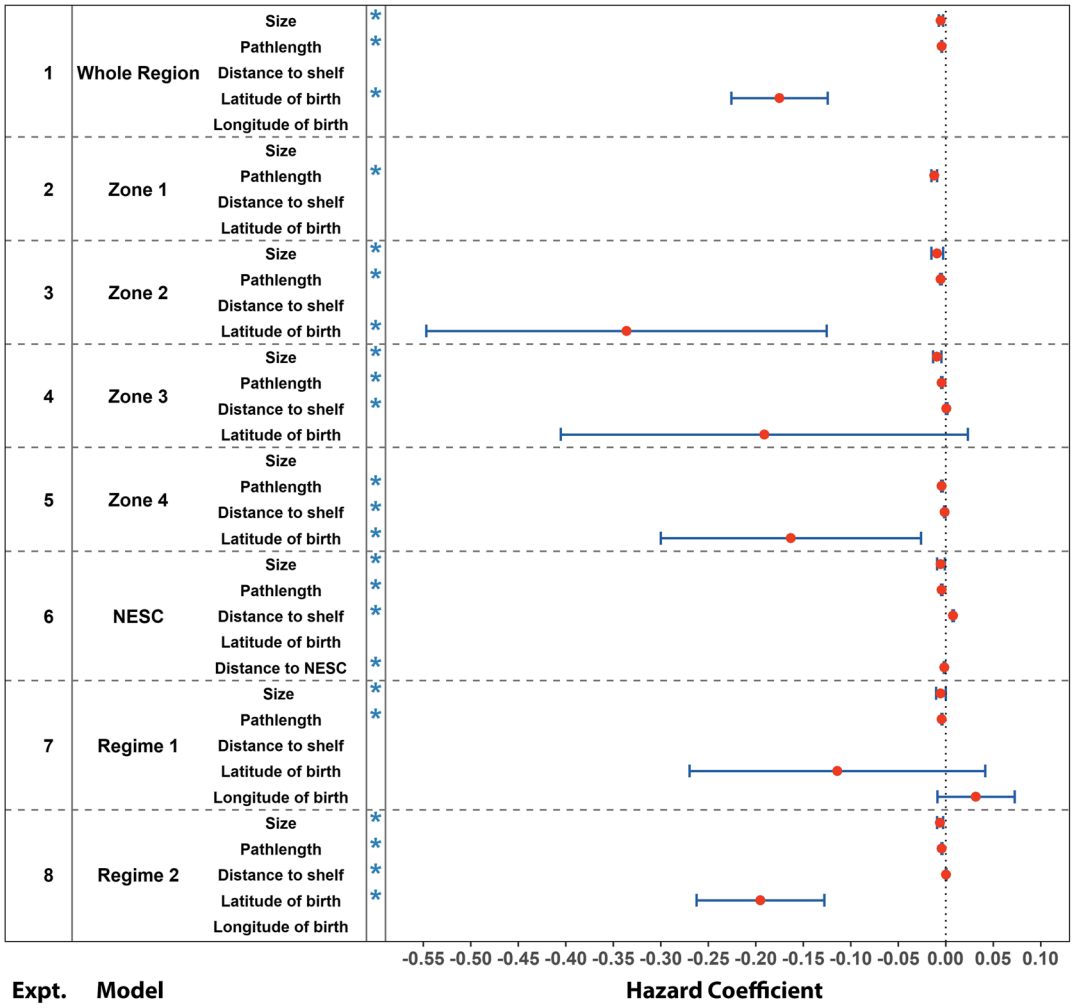

Figure 4. Results from the Cox model analysis in eight experiments identified by their model scenarios (second left column). Hazard coefficients of explanatory variables for each Cox proportional hazard model scenario is shown on the right. Blue stars indicate the hazard coefficients that are significant (p value < 0.05). Variables missing a plotted point denote variables that were not selected by the model. Error bars indicate the 95% confidence intervals of the coefficients.

$$log(h_i(t|\mathbf{x}_i)) = log(h_0(t)) + \boldsymbol{\beta}\mathbf{x}_i. \tag{6}$$

The following explanatory variables representing hazards (or covariates $\mathbf{x}_i$ in Equation 6) were included in the model estimation.

- Size, or the equivalent radius (R) of a WCR, where πR^2 = area of the WCR.
- The distance of movement during the life of a WCR, where this distance is measured between WCR formation and demise locations, called the "pathlength".
- The zonal distance of WCR formation location to the continental shelf break.
- Longitude and latitude of formation location.

A total of eight model scenarios or experiments were performed to conduct the Cox PH analysis (see Figure 4, left column). These experiments included (i) a total of five zonal classifications of the GS and the Slope Sea region; (ii) positioning of New England Seamount Chain (NESC); and (iii) two regimes identified before and after the year 2000 (Regimes 1 and 2, respectively). Each experiment included the covariates indicated above as appropriate. For example, Experiment 3 sets up the Cox model with lifespans of WCRs in Zone 2 as the response variable (right-hand side of Equation 6) and four hazard covariates ($\mathbf{x}_i$ on the right side of Equation 6) given by size, pathlength, distance to shelf, and formation latitude. The idea is to assess the

risk of failure of the lifespan against the four hazards (covariates). The variable longitude of WCR formation was only included in the model scenarios that considered the entire GS region (Experiments 1, 7, and 8) and excluded from the zonal category models (Experiments 2–5) and the NESC model (Experiment 6). For this study, the pathlength was computed based on the direct geographical distance between the locations of formation and demise (unfortunately, an approximation of the real trajectory), leaving an option to improve in later studies.

For simplicity, the NESC was included in the survival analysis models as a north-south barrier at 62.5° W. The zonal distance was calculated to the NESC from each WCR formed to the east of the barrier. We then used this distance as a covariate and estimated the Cox model only for the WCRs east of the NESC to investigate the effects of distance to NESC from WCR formation locations on their survival.

All selected explanatory variables (covariates $\mathbf{x}_i$ in Equation 6) for the Cox model analysis were continuous variables. In a broader Cox modeling context, the categorical variables such as the season of formation, the season of demise, the zone of formation, and the zone of demise were exempted from the model since initial analyses found these categorical variables contained the same information as the continuous variables. These were the essential categories in our survival analysis methodology in the first step. It was expected that covariates included in the Cox PH model met the model assumptions. These assumptions include (i) linear contribution to the model by covariates when lifespan is the response variable, (ii) independence of survival times (i.e., independence of WCR lifespans), and (iii) constant hazard ratio over time. The first assumption quantifies the relationship between the logarithm of the hazard function and the covariates as a linear function (see Equation 6). The assumption of constant hazard ratio over time is an important feature in the Cox model and is also known as the PH assumption. In simple terms, the PH assumption states the ratio of the hazard functions for two WCRs with different regression vectors does not vary with time (Ng'andu, 1997). When considering the assumption of "independence of survival times", we assumed that the ring-ring interactions of WCRs were random. We also assumed time invariance within regimes and helped meet our assumption by separating the analysis into the regime time periods identified.

To find the set of covariates that provided the most parsimonious fits to the observed WCR survival data, backward model selection using Akaike's information criterion (AIC) (Akaike, 1974) was used for each scenario. Based on the AIC values of the backward selection method and p values of the model output, the best covariates for the model were identified. Model validation was conducted based on model fits and inspection of deviance residuals. Together with Figure 4 and Equations 4–6, this completes the second step of the two-step survival analysis process. The results are presented and analyzed in section 4 later.

3. Survival Function of WCRs

The WCRs formed in Zone 2 had a higher survival probability with age in comparison to the other three zones (Figure 2a). To reach the 50% probability, the WCRs formed in Zone 2 took more than 60 days while the WCRs formed in Zones 1, 4, and 3 took 30, 35, and 45 days, respectively. This finding was supported by the log-rank test conducted, which rejected the null hypothesis, H_0 (all survival curves are the same) at the $\alpha = 0.05$ level ($p < 0.05$).

Comparing the different zones from a demise perspective, the WCRs that demised in Zone 1 had a higher survival probability (longer lifespan) (Figure 2b). Half the WCRs last documented in Zone 1 lived for more than 85 days while only half the WCRs last documented in the other three zones lived longer than 50 days. This result was supported by a log-rank test that rejected the H_0 ($\alpha = 0.05$, $p < 0.05$).

Seasonally, the WCRs formed during the winter had the highest survival (Figure 2c) (p value was 0.04, rejecting H_0). Interannually, a comparison of the survival probability between the WCRs in the two regimes (Regime 1 is 1980–1999, and Regime 2 is 2000–2017) shows WCRs formed in the earlier regime had a higher survival probability than those formed in the later regime (Figure 2d). This was supported by the log-rank test, which showed the difference was statistically significant ($\alpha = 0.05$, $p < 0.05$).

The WCRs exhibited a higher survival rate when formed in Zone 2 compared to other zones and similarly when demised in Zone 1 compared to in other zones (cf. Figures 2a and 2b). This motivated us to investigate the survival probability by binning WCRs into different formation and demise zone combinations (Figure 3). Combinations Z3Z1 (Curve H in Figure 3) and Z2Z1 (Curve G in Figure 3) have the highest survival probability of all the different combinations. The G and H combinations reached 50% survival probability at 140 and

225 days, respectively. Lower survival probability was shown by Curves E and F (Figure 3) with a half-life time of 75 days. The lowest of all the survival probabilities were the WCRs formed and demised in the same region (A, B, C, and D) with the 50% probability at 30 to 40 days. The statistically significant difference between these survival curves was evident when a log-rank test was carried out ($\alpha = 0.05, p < 0.05$). It is evident that *Z*2*Z*1 rings have a higher survival probability compared to the rest of the WCRs ($\alpha = 0.05, p < 0.05$). Half the *Z*2*Z*1 rings lived at least 140 days (Figure 3). For other categories, this half-life was around 40 days. Not only this combination has higher probability compared to other rings formed in Zone 2, it also has a higher probability than all rings that cross a zone. Survival curves for combinations Z4Z1 and Z4Z2 are not included in Figure 3 due to their low number of rings (8 for Z4Z1 and 5 for Z4Z2).

4. Cox PH Model Analysis

Figure 4 presents the estimated hazard coefficients and their 95% confidence intervals of the Cox PH analysis conducted on multiple scenarios for the models selected by AIC. It also indicates the significance of these coefficients. In the whole region scenario, WCR size, pathlength, and latitude of formation affected the survival of the WCRs. These hazard coefficients are obtained as negative, which implies that increasing values of these variables decrease the impact of the total hazard on the survival of a WCR. In other words, increasing values of these variables increase the survival probability of WCRs. Size and pathlength coefficients were close to zero while the latitude of formation had a higher coefficient (−0.175). When a Cox model was fitted for WCRs formed in Zone 1, the only significant and selected variable included in the best model was pathlength. The hazard coefficient for pathlength was very close to zero (−0.008) in this scenario. Similar to the whole GS scenario, size, pathlength, and formation latitude were included in the best model when analyzing WCRs formed only in Zone 2. Similarly, size and pathlength had negative hazard coefficients closer to zero while formation latitude coefficient was −0.336.

For WCRs formed in Zone 3, significant variables for survival included in the best model were size, pathlength, and distance to the shelf where every hazard coefficient of these variables had a value near zero. Of these hazard coefficients, the only positive value was the distance to shelf. For WCRs formed in Zone 4, the best model did not include the "size" variable, while all the other variables were accepted and were significant. Both hazard coefficients for pathlength and distance to shelf were negative and near-zero values (−0.004, −0.001) while latitude of formation had a hazard coefficient of −0.163. It is interesting to observe how the sign of distance to shelf hazard coefficient switched from positive to negative when comparing the Zones 3 and 4 models.

In the NESC scenario (where only WCRs formed to the east of the New England Seamount Chain were analyzed), the "distance to NESC" had a negative hazard coefficient which implies that forming farther to the east from the NESC results in a higher survival probability in the WCRs.

When a comparison between the WCRs that were formed in the two regimes was conducted using the Cox model output for each regime scenario, size and pathlength were found to be the significant variables for WCR survival in both regimes. Latitude of formation was not a significant variable for WCR survival in Regime 1 whereas it was included in the model for Regime 2. Latitude of formation appeared to have a significant hazard coefficient for WCR survival in multiple scenarios. Also, the switching of signs in the hazard coefficient for distance to shelf between Zones 3 and 4 suggests the effect of the NESC between these regions, which is discussed below.

5. Discussion

It is well known that WCRs generally propagate westward as a nonlinear manifestation of the same process that supports Rossby waves (Olson, 1991), so one would expect that rings formed in Zones 3 and 4, being further away from the shelf break, would live longer than those formed in Zone 1 or 2. WCRs formed in Zone 2 had a higher survival probability than those formed in the other three zones. When examining the WCR demise zone effect on survival probabilities, we discovered that WCRs that demised in Zone 1 had a higher survival probability than WCRs that demised in the rest of the zones. An important pattern emerged that relates the WCR trajectories to the survival time. We note that multiple WCRs formed in Zone 2 showed a migration path along the shelf and propagate westward toward Zone 1 and had a longer life span. There were 82 rings that showed this pattern of long-lived propagation (Z2Z1 WCRs). A similar pattern was seen for rings that were formed in Zone 3 and demised in Zone 1 (Z3Z1). A number of factors might be responsible

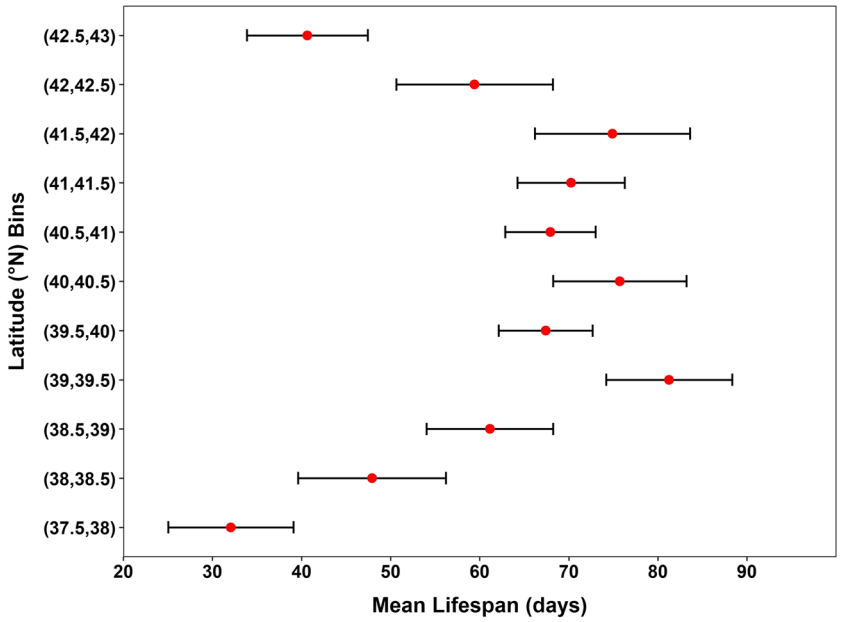

Figure 5. Mean lifespan of WCRs formed in different 0.5° latitudinal bands between 37.5° N and 43° N. Error bars indicate standard error of the mean lifespan.

for this unique result. First, WCRs formed in Z1, being in close proximity to the shelf, encounter the shelf break within a few weeks of their westward propagation. Second, WCRs formed in Z4 encounter the New England Seamount Chain as they propagate westward. How exactly the life spans of WCRs in Z3 and Z4 get shortened due to their interaction with the NESC requires more dynamical and numerical studies in the future. On the other hand, WCRs formed in Zone 2 and many in Zone 3 do not interact with the NESC and have enough space to the west to propagate for a long time. The trajectories of Z2Z1 and Z3Z1 WCRs should be further investigated for understanding how WCRs might affect the continental shelf circulation and associated ecosystem.

Seasonally, WCRs formed in the winter survived the longest (Figure 2c). There are two possible explanations. First, winter is in general, a low-productivity period for WCR formation; fewer WCRs are formed from the GS during this period. So fewer rings formed in the winter reduce the chance of interactions or GS meanders before the GS becomes very energetic in the spring and summer when the slope water space is crowded with multiple energetic features (meandering stream and multiple rings cohabitating the same general area). Second, the WCRs formed in the winter undergo convection (Schmitt & Olson, 1985). This reduces the stratification and will reduce the radius of deformation (R_d). A smaller (reduced R_d) ring would be less likely to be reabsorbed by the stream. In contrast, rings in other seasons formed with higher initial stratification (Auer, 1987; Hogg & Johns, 1995) would have larger R_d and a greater probability of interacting with the meanders and the continental shelf. This possibility needs further investigation in a dynamical framework in the future.

When WCR survival probabilities were compared between the two regimes, we found that the survival of WCRs has decreased from the previous regime (1980–1999) to the later regime (2000–2017). This result agrees with the reduced mean lifespan median values of WCRs in Regime 2 (see Gangopadhyay, Gawarkiewicz, Silva, et al., 2020, Tables 3 and 4). Two factors might have led to this result. First, Regime 2 showed considerably higher ring frequency (annual average of 33 rings in the later regime compared to 18 in the previous regime; see Gangopadhyay et al., 2019), which might have increased the hazard of rings in Regime 2 to propagate to the shelf break. Second, since Regime 2 is in a time period of rapid warming (Chen et al., 2020; Forsyth et al., 2015; Gawarkiewicz et al., 2018), the ring waters during this time would generally be more stratified than those in Regime 1. The interplay of factors such as stratification, size, and radius of deformation at formation is a complex dynamical process which is further affected by air-sea fluxes during the lifetime of a ring and open opportunities for new research. Future studies will also focus on the causes of regime shift for the annual formation rate of WCRs and implication for the survival of rings.

Results of the Cox models for different scenarios clearly indicate that the latitude of formation, size of the WCR, and the distance a WCR propagated are major covariates that affected the survival of WCRs. Rings that are formed at more northerly latitudes survived longer (Figure 5). WCRs formed to the south of 37.5° N and the north of 43° N were not included for the average lifespan calculation, since there were only a few rings which resulted in lower degrees of freedom. WCRs reported in the first bin (37.5–38° N) only formed in Zone 1 and WCRs reported in the last bin (42.5°–43° N) were only formed in Zone 4. WCRs formed in the lower latitudes naturally interact more with the GS meanders and have a lower survival rate. WCRs formed in the higher latitudes have a higher chance of colliding with the shelf break as they travel westward and thus have a lower survival probability (and higher hazard) as well. Higher hazard coefficient values of the formation latitude effect may be expressing that WCRs formed further from the time-mean GS path had lower probabilities of being reabsorbed to the GS soon after formation.

The higher eddy kinetic energy in larger WCRs may be a reason why WCR survival is positively correlated with the equivalent radius. In Zone 1 the only WCR variable that had a significant effect on survival was the distance a WCR moved. The size factor was not significant in Zone 1 since there is a very small size variability in Zone 1 WCRs (Silva, 2019). Also, the latitudinal variability is very small in Zone 1. Interestingly, on top of the distance propagated, size and formation latitude became significant on survival when WCRs formed in Zone 2. In Zone 3, distance to shelf had a negative significant effect on WCR survival in addition to the significance of WCR size and pathlength. We believe this negative effect from the distance to shelf is correlated with the proximity to the NESC of Zone 3 WCRs (Cornillon, 1986). Therefore, we specifically checked this using a north-south longitude barrier at 62.5° W as the NESC factor and ran the Cox model for the WCRs east of NESC. As expected, proximity to NESC had a negative effect on WCR survival. In summary, there exist covariances between the explanatory variables used in the set of Cox models. Thus, the effect on WCR survival from these variables is more aggregated and complex than a simple linear effect. This suggests opportunities for alternative analyses and a detailed investigation of the cause-effect direction for the response variable and some of the covariates.

6. Conclusions

This study presents an overview of GS's WCR survival based on multiple survival analysis techniques applied. A comparison between the survival probability of WCRs in separate longitudinal zones of the GS was followed by Cox PH analysis. The major results of this study are listed below.

- WCRs formed in Zone 2 had a higher survival probability compared to the WCRs formed in the rest of the three zones.
- WCRs last seen or demised in Zone 1 had a higher survival probability.
- WCRs which were formed in winter had a higher survival probability than WCRs formed in the other three seasons.
- Survival probability of WCRs formed in Zone 2 or 3 and demised in Zone 1 was higher than any other formation and demisal zone combination.
- Survival probability increased to more than 70% for WCRs formed within a latitude band of 39.5° to 41.5°.
- Radius and propagation distance are significant factors affecting the survival of WCRs.
- Among the WCRs which formed to the east of the NESC, rings that formed farther from the NESC had higher survival probability.

The complex nature of the impact of different variables on the survival of a WCR is evident in our analysis presented. The results highlight the need for aggregated and spatial analysis for further understanding the causality of survival of WCRs.

Future work using WCR survival analysis could be used to estimate probable WCR-shelf interactions in a given shelf-species spawning season. The derived survival probabilities in this study could then be used to estimate the likelihood of WCRs hitting the shelf, which in turn could predict the species recruitment.

Data Availability Statement

The WCR Census data (1980–2017) are available through the Biological and Chemical Oceanography Data Management Office (https://www.bco-dmo.org/dataset/810182).

Acknowledgments
We are greatly indebted to the large number of scientists, researchers, and fishermen who have gone to sea to observe, document, and understand the Gulf Stream warm core rings and cold core rings over the last 40 years, without which creating the census would never have been possible. We gratefully acknowledge the efforts of NOAA and NASA for their satellite observations, which helped developed the synoptic Gulf Stream and ring analysis charts. These Gulf Stream analysis charts compiled by Jenifer Clark (coauthor) and Roger Pettipas were used to develop the original census, which was started by M. Monim and followed by coauthors N. Silva and A. Silver. We have benefited from many discussions on GS system behavior and variability with Tom Rossby, Charlie Flagg, Kathy Donohue, Randy Watts, Peter Cornillon, and Magdalena Andres. We are grateful for financial supports from NOAA (NA11NOS0120038), NSF (OCE-1851242), SMAST, and UMass Dartmouth. G. G. was supported by NSF under grant OCE-1851261. N. S. would also like to acknowledge the help from Dr. Andre Schmidt of SMAST with computational issues and the support of the Department of Earth and Environment of Boston University. We wish to thank the Editor and three anonymous reviewers for their helpful comments and encouragement to a previous version which improved the focus of this manuscript.

References

Akaike, H. (1974). A new look at the statistical model identification, *Selected papers of hirotugu akaike* (pp. 215–222). New York: Springer.
Auer, S. J. (1987). Five-year climatological survey of the Gulf Stream system and its associated rings. *Journal of Geophysical Research*, *92*(C11), 11,709–11,726. https://doi.org/10.1029/JC092iC11p11709
Bisagni, J. J. (1976). Passage of anticyclonic Gulf Stream eddies through Deepwater Dumpsite 106 during 1974 and 1975 (*76–1*): National Oceanic and Atmospheric Administration.
Bisagni, J. J. (1983). Lagrangian current measurements within the eastern margin of a warm-core Gulf Stream ring. *Journal of Physical Oceanography*, *13*(4), 709–715. https://doi.org/10.1175/1520-0485(1983)013<0709:LCMWTE>2.0.CO;2
Bisagni, J. J., Gangopadhyay, A., & Sanchez-Franks, A. (2017). Secular change and inter-annual variability of the Gulf Stream position, 1993-2013, 70°–55° W. *Deep Sea Research Part I: Oceanographic Research Papers*, *125*, 1–10. https://doi.org/10.1016/j.dsr.2017.04.001
Brown, O. B., Cornillon, P. C., Emmerson, S. R., & Carle, H. M. (1986). Gulf Stream warm rings: A statistical study of their behavior. *Deep Sea Research Part A.Oceanographic Research Papers*, *33*(11–12), 1459–1473. https://doi.org/10.1016/0198--0149(86)90062--2
Brown, O. B., Olson, D. B., Brown, J. W., & Evans, R. H. (1983). Satellite infrared observations of the kinematics of a warm-core ring. *Marine and Freshwater Research*, *34*(4), 535–545.
Chen, Z., Kwon, Y.-O., Chen, K., Fratantoni, P., Gawarkiewicz, G., & Joyce, T. M. (2020). Long-term SST variability on the northwest Atlantic continental shelf and slope. *Geophysical Research Letters*, *47*, e2019GL085455. https://doi.org/10.1029/2019GL085455
Churchill, J. H., Cornillon, P. C., & Milkowski, G. W. (1986). A cyclonic eddy and shelf-slope water exchange associated with a Gulf Stream warm-core ring. *Journal of Geophysical Research*, *91*(C8), 9615–9623.
Clark, T. G., Bradburn, M. J., Love, S. B., & Altman, D. G. (2003). Survival analysis Part I: Basic concepts and first analyses. *British journal of cancer*, *89*(2), 232–238.
Cornillon, P. (1986). The effect of the New England Seamounts on Gulf Stream meandering as observed from satellite IR imagery. *Journal of Physical Oceanography*, *16*(2), 386–389. https://doi.org/10.1175/1520-0485(1986)016<0386:TEOTNE>2.0.CO;2
Cowen, R. K., Hare, J. A., & Fahay, M. P. (1993). Beyond hydrography: Can physical processes explain larval fish assemblages within the Middle Atlantic Bight?. *Bulletin of Marine Science*, *53*(2), 567–587.
Cox, D., & Oakes, D. (1984). *Analysis of survival data*. London: Chapman & Hall.
Csanady, G. T. (1979). The birth and death of a warm core ring. *Journal of Geophysical Research: Oceans*, *84*(C2), 777–780. https://doi.org/10.1029/JC084iC02p00777
Davis, C. S., & Wiebe, P. H. (1985). Macrozooplankton biomass in a warm-core Gulf Stream ring: Time series changes in size structure, taxonomic composition, and vertical distribution. *Journal of Geophysical Research*, *90*(C5), 8871–8884.
Decker, B. L. O. U. I. S. (1986). World geodetic system 1984: Defense Mapping Agency.
Flierl, G. R. (1977). The application of linear quasigeostrophic dynamics to Gulf Stream rings. *Journal of Physical Oceanography*, *7*(3), 365–379. https://doi.org/10.1175/1520-0485(1977)007<0365:TAOLQD>2.0.CO;2
Flierl, G. R., & Wroblewski, J. S. (1984). The possible influence of warm core Gulf Stream rings upon shelf water larval fish distribution. *Fishery Bulletin- National Oceanic and Atmospheric Administration*, *83*, 313–330.
Forsyth, J. S. T., Andres, M., & Gawarkiewicz, G. G. (2015). Recent accelerated warming of the continental shelf off New Jersey: Observations from the CMV Oleander expendable bathythermograph line. *Journal of Geophysical Research: Oceans*, *120*, 2370–2384. https://doi.org/10.1002/2014JC010516
Gangopadhyay, A., Chaudhuri, A. H., & Taylor, A. H. (2016). On the nature of temporal variability of the Gulf Stream path from 75° to 55° W. *Earth Interactions*, *20*(9), 1–17. https://doi.org/10.1175/EI-D-15-0025.1
Gangopadhyay, A., & Gawarkiewicz, G. (2020). Yearly census of Gulf Stream warm core ring formation from 1980 to 2017. Biological and Chemical Oceanography Data Management Office (BCO-DMO), Dataset version 2020-05-06, https://doi.org/10.26008/1912/bco-dmo.810182.1
Gangopadhyay, A., Gawarkiewicz, G., Silva, E. N. S., Monim, M., & Clark, J. (2019). An observed regime shift in the formation of warm core rings from the Gulf Stream. *Scientific Reports*, *9*(1), 1–9. https://doi.org/10.1038/s41598-019-48661-9
Gangopadhyay, A., Gawarkiewicz, G., Silva, E. N. S., Silver, A. M., Monim, M., & Clark, J. (2020). A census of the warm-core rings of the Gulf Stream: 1980–2017. *Journal of Geophysical Research: Oceans*, *125*, e2019JC016033. https://doi.org/10.1029/2019JC016033
Gaube, P., & McGillicuddy, D. J. (2017). The influence of Gulf Stream eddies and meanders on near-surface chlorophyll. *Deep Sea Research Part I: Oceanographic Research Papers*, *122*, 1–16.
Gawarkiewicz, G., Bahr, F., Beardsley, R. C., & Brink, K. H. (2001). Interaction of a slope eddy with the shelfbreak front in theMiddle Atlantic Bight. *Journal of Physical Oceanography*, *31*(9), 2783–2796. https://doi.org/10.1175/1520-0485(2001)031<2783:IOASEW>2.0.CO;2
Gawarkiewicz, G., Todd, R. E., Zhang, W., Partida, J., Gangopadhyay, A., Monim, M.-U.-H., et al. (2018). The changing nature of shelf-break exchange revealed by the OOI Pioneer Array. *Oceanography*, *31*(1), 60–70. https://doi.org/10.5670/oceanog.2018.110
Halliwell, G. R., & Mooers, C. N. K. (1979). The space-time structure and variability of the shelf water-slope water and Gulf Stream surface temperature fronts and associated warm-core eddies. *Journal of Geophysical Research*, *84*(C12), 7707–7725. https://doi.org/10.1029/JC084iC12p07707
Hare, J. A., Churchill, J. H., Cowen, R. K., Berger, T. J., Cornillon, P. C., Dragos, P., et al. (2002). Routes and rates of larval fish transport from the southeast to the northeast United States continental shelf. *Limnology and Oceanography*, *47*(6), 1774–1789.
Hogg, N. G., & Johns, W. E. (1995). Western boundary currents. *Reviews of Geophysics*, *33*(S2), 1311–1334.
Joyce, T. M. (1985). Gulf Stream warm-core ring collection: An introduction. *Journal of Geophysical Research*, *90*(C5), 8801–8802. https://doi.org/10.1029/JC090iC05p08801
Joyce, T. M., & McDougall, T. J. (1992). Physical structure and temporal evolution of Gulf Stream warm-core ring 82B. *Deep Sea Research Part A.Oceanographic Research Papers*, *39*, S19–S44. https://doi.org/10.1016/S0198-0149(11)80003-8
Joyce, T. M., & Wiebe, P. (1983). Warm-core rings of the Gulf Stream. *Oceanus*, *26*(2), 34–44.
Kaplan, E. L., & Meier, P. (1958). Nonparametric estimation from incomplete observations. *Journal of the American Statistical Association*, *53*(282), 457–481. https://doi.org/10.2307/2281868
Kleinbaum, D. G., & Klein, M. (2012). *Survival analysis*, Statistics for Biology and Health (3rd ed.). New York: Springer. Retrieved from https://www.springer.com/gp/book/9781441966452
Lai, D. Y., & Richardson, P. L. (1977). Distribution and movement of Gulf Stream rings. *Journal of Physical Oceanography*, *7*(5), 670–683. https://doi.org/10.1175/1520-0485(1977)007<0670:DAMOGS>2.0.CO;2
McCarthy, J. J., & Nevins, J. L. (1986). Sources of nitrogen for primary production in warm-core rings 79-E and 81-D. *Limnology and Oceanography*, *31*(4), 690–700.

Monim, M. (2017). Seasonal and inter-annual variability of Gulf Stream warm core rings from 2000 to 2016 (Master's Thesis), University of Massachusetts Dartmouth, USA.
Myers, R. A., & Drinkwater, K. (1986). The effects of entrainment of shelf water by warm core rings on Northwest Atlantic fish recruitment. *ICES CM*, *100*, 13.
Ng'andu, N. H. (1997). An empirical comparison of statistical tests for assessing the proportional hazards assumption of Cox's model. *Statistics in medicine*, *16*(6), 611–626.
Olson, D. B. (1991). Rings in the ocean. *Annual Review of Earth and Planetary Sciences*, *19*(1), 283–311.
QGIS Development Team (2016). QGIS geographic information system.
R Core Team (2018). R: A language and environment for statistical computing. R Foundation for Statistical Computing, Vienna, Austria, https://www.R-project.org/
Ramp, S. R., Beardsley, R. C., & Legeckis, R. (1983). An observation of frontal wave development on a shelf-slope/warm core ring front near the shelf break south of New England. *Journal of Physical Oceanography*, *13*(5), 907–912. https://doi.org/10.1175/1520-0485(1983)013<0907:AOOFWD>2.0.CO;2
Saunders, P. M. (1971). Anticyclonic eddies formed from shoreward meanders of the Gulf Stream. *Deep Sea Research and Oceanographic Abstracts*, *18*(12), 1207–1219. https://doi.org/10.1016/0011-7471(71)90027-1
Schmitt, R. W., & Olson, D. B. (1985). Wintertime convection in warm-core rings: Thermocline ventilation and the formation of mesoscale lenses. *Journal of Geophysical Research*, *90*(C5), 8823–8837.
Silva, E. N. S. (2019). *Understanding thirty-eight years of Gulf Stream's warm core rings: Variability, regimes and survival* (MS Thesis). (125 pp.). University of Massachusetts Dartmouth.
Smith, W. G., Pennington, M., Berrien, P., Sibunka, J., Konieczna, M., Baranowski, M., & Meller, E. (1979). Annual changes in the distribution and abundance of Atlantic cod and haddock larvae off the northeastern United States between 1973–74 and 1977–78. *ICES CM*, *6*, 47.
Therneau, T. M. (2015). A package for survival analysis in S. https://CRAN.R-project.org/package=survival, version 2.38.
Wiebe, P. H., Flierl, G. R., Davis, C. S., Barber, V., & Boyd, S. H. (1985). Macrozooplankton biomass in Gulf Stream warm-core rings: Spatial distribution and temporal changes. *Journal of Geophysical Research*, *90*(C5), 8885–8901.